



Monitoring land use change of Meyjaran Dam area before and after construction using remote sensing and GIS techniques

Mojtaba Golbaf¹ , Farbod Papoli Yazdi² , and Fereshteh Modaresi²

¹Department of Remote Sensing, Faculty of Earth Sciences, Shahid Beheshti University, Tehran, Iran

²Department of Water Science and Engineering, Faculty of Agriculture, Ferdowsi University of Mashhad, Mashhad, Iran

ARTICLE INFO	ABSTRACT
<p>Paper Type: Research Paper</p> <p>Received: 27 December 2024 Revised: 31 March 2025 Accepted: 07 April 2025 Published: 08 April 2025</p> <p>Keywords Meyjaran Dam Land Use Changes Location Quotient Index Maximum Likelihood Supervised Classification</p> <p>Corresponding author: F. Modaresi ✉ fmodaresi@um.ac.ir</p>	<p>The construction of large dams in regions with temperate climates and dense forest cover causes significant land use changes that require precise assessment and continuous monitoring. To prevent the worsening of crises related to vegetation degradation and the loss of natural resources, the cumulative impacts of dam construction must be evaluated over time using a hydro-ecological approach. This study investigates land use and vegetation cover changes in the Meyjaran Dam basin over 30 years. Satellite imagery from Landsat 5 and Sentinel-2B was employed to assess the pre- and post-construction periods. Land use changes were analyzed in two spatial extents: a small study area (464 ha) and a larger watershed (4,027 ha) that includes the study area and the upstream dense forest cover. Image classification was performed using supervised classification with the Maximum Likelihood algorithm, achieving a Kappa coefficient of 0.99. Spatial change analysis was conducted using the Location Quotient (LQ) index. The results indicated that within the small study area, forest cover declined by 84.22 ha (18.14%), while built-up areas increased by 25.25 ha, and rangelands and agricultural lands grew by 24.19 ha. In the larger watershed, forest cover decreased by 120.80 ha (3%). These findings highlight the extensive ecological impacts of dam construction on forest ecosystems beyond the immediate inundation zone.</p>
<p>Highlights</p> <ul style="list-style-type: none"> • Examined land use changes before and after dam construction • LQ index shows 18% forest loss in a small watershed, indicating the dam's direct impact. • Forest cover reduction in the large watershed shows broader impacts beyond the area of inundation. • Image classification results, with a high Kappa coefficient (0.99 for 2021), confirm the method's accuracy. 	
<p>How to cite this paper: Golbaf, M., Papoli Yazdi, F., & Modaresi, F. (2025). Monitoring land use change of Meyjaran Dam area before and after construction using remote sensing and GIS techniques. <i>Environment and Water Engineering</i>, 11(2), 155-164. https://doi.org/10.22034/ewe.2025.494716.1992</p>	

1. Introduction

Nowadays, to meet diverse demands for welfare, economic development, and agricultural productivity, the construction of dams with various purposes, such as the supply of drinking water, irrigation, flood control, hydropower generation, tourism, and aquaculture, has significantly increased (Linh et al., 2025). However, despite their short-term advantages, dams can exert long-term impacts on the environment and surrounding land use patterns, necessitating careful assessment (Yu et al., 2024). From the early phases, dam construction projects affect environmental resources, such that the formation of large reservoirs in vegetated areas can result

in the destruction of wildlife habitats and plant resources (Castro-Diaz et al., 2024). Furthermore, these projects cause noticeable changes in land use patterns. For example, studies have shown that the construction and impoundment of the Alborz Dam significantly impacted vegetation cover and land use in both upstream and downstream areas (Darikandeh et al., 2020).

The technical and economic limitations of traditional surveying methods have made the use of modern remote sensing and geographic information systems indispensable in land use studies. These technologies provide a comprehensive view and enable periodic monitoring, offering a more precise

analysis of environmental change trends. Case studies in the Yellow River watershed, utilizing satellite imagery and the Markov chain model, have accurately predicted land use change patterns (Rezaei et al., 2023). Similarly, studies in the Doroodzan Dam watershed indicate increasing trends in barren lands, agricultural areas, and residential zones by the year 2050, at the expense of declining rangelands and forested areas (Zarei et al., 2024). The analysis of the Tehri Dam in India revealed significant changes in over 2,600 ha of agricultural land and drastic transformations in 3,347 ha of land surrounding the reservoir. A similar pattern was observed at the Taleghan Dam, where vegetation degradation and expansion of residential and recreational zones shaped prominent regional transformations (Motkan et al., 2010).

Research shows that the construction of the Alborz Dam between 1994 and 2016 led to an increase of 22.7 ha in forest vegetation and a reduction of 735.66 ha in rangeland and agricultural land, while the dam and reservoir covered approximately 530 ha (Darikandeh et al., 2020). Additionally, land cover change assessments in the Ardabil region between 1986 and 2016 revealed the loss of approximately 60,127 ha of rainfed cropland and 1,701 ha of rangeland (Namdar et al., 2021). Recent studies on the ecological effects of dam construction show significant structural transformations in regional ecosystems. Investigations around the Hali Dam constructed in 2009 in a region with an arid climate and annual precipitation of 50 to 100 mm demonstrated a sharp decline in vegetation cover following reservoir impoundment, particularly during dry seasons. These changes showed a strong correlation with water accumulation patterns in the reservoir and the expansion of irrigated agriculture (Almalki et al., 2023). A noteworthy finding of this study was the alteration of the region's natural ecological interactions. Statistical analyses indicated a decline in vegetation sensitivity to climatic factors from 85% before to 42% after dam construction highlighting a fundamental disruption in the ecosystem's natural cycles.

On a broader scale, monitoring 137 major dams across China over a 28-year period enabled the precise identification of long-term vegetation change trends and disturbances due to human intervention (He et al., 2024). Field studies in the Gaborone Dam watershed in Botswana revealed substantial land use and land cover changes related to water resources. The study recorded an 8.9% decrease in vegetation cover, coinciding with an equivalent increase in bare soil area. Additionally, built-up areas increased by 2.49%, while agricultural land decreased by 2.8% (Ouma et al., 2024). Domestically, land use monitoring in the Zarand region of Kerman over the past three decades showed a remarkable expansion of orchards by 2,893 ha and a reduction of barren lands by 1,573 ha (Sanjari et al., 2013). These trends align with findings by researchers such as Thakkar et al. (2017). A key point in satellite image-based studies is the necessity of using same-season data (preferably summer) for comparative vegetation cover analysis, as this minimizes seasonal variation errors and enhances result validity.

Accurate prediction of land use change trends plays a critical role in sustainable water resource management. This study aims to monitor and analyze these changes in the Meyjaran Dam watershed over a 30-year period, encompassing both the

pre- and post-construction phases of the dam. To achieve this objective, Landsat 5 satellite data were processed for the pre-construction period, while Sentinel-2B imagery was utilized to represent current conditions (2021). This analytical approach enabled the identification and quantitative assessment of the environmental impacts of the dam, the most significant of which include changes in forest cover, expansion of residential and industrial areas, and transformations in the region's water resource patterns. The application of remote sensing technology in this study offers several advantages over traditional methods. Continuous and comprehensive monitoring of the study area over a three-decade period has allowed for the detection of long-term change trends that would be difficult to observe through field-based methods alone.

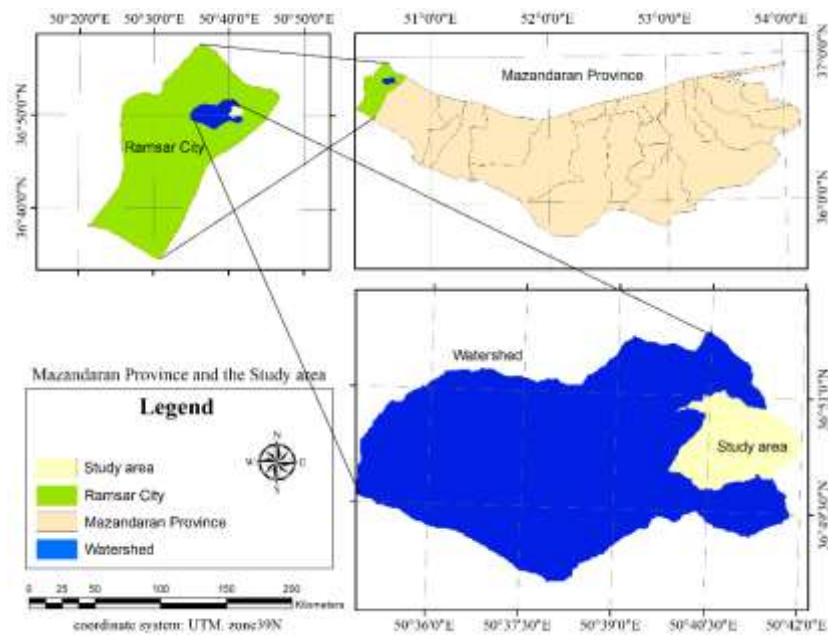
Furthermore, the use of supervised classification techniques combined with accuracy assessment through the Kappa coefficient has significantly enhanced the reliability of the results. The integration of satellite data with Geographic Information System (GIS) tools enabled the generation of detailed maps and advanced spatial analyses using indicators such as the Location Quotient (LQ). The use of multi-source satellite data has facilitated the examination of long-term changes, while the application of the LQ index has allowed for precise spatial change analysis. Additionally, classification accuracy assessment through the Kappa coefficient ensures the credibility of the findings. A notable aspect of this study is the selection of a region with a humid climate and rich vegetation—an area that, unlike arid regions, has received comparatively less attention in dam-related research. The main objective of this research is to investigate the relationship between changes in vegetation cover and land use with the construction and operation of the Meyjaran Dam. To achieve this aim, remote sensing techniques have been employed to collect and analyze accurate and reliable data on these changes.

2. Materials and Methods

2.1 Study area

In this study, the area investigated includes the lake and associated lands of the Meyjaran Dam, as well as the watershed that drains into the dam. This area lies within the approximate geographical coordinates of 50° 36'E to 50° 42'E longitude and 36° 47'N to 36° 51'N latitude, in Iran. The Meyjaran Dam is an earth-fill dam with an asphaltic core, the construction of which began in 1993 on the Nesarood River in Ramsar County, Mazandaran Province, located between the mountains of Erbe-Kaleh and Dalkhani, Iran. The dam has a storage capacity of 8 MCM. Figure 1 illustrates the geographical extent of the Meyjaran Dam watershed in Mazandaran Province. This map delineates the location of the dam, dense forest areas, agricultural lands, rangelands, and surrounding residential zones using satellite data and a Digital Elevation Model (DEM). The study area is divided into two parts: a small basin (study area) and a larger watershed. The small basin, shown in yellow in Fig. 1, has an approximate area of 464 ha and includes land adjacent to the dam in all four directions. The large watershed, shown in blue, covers an area of approximately 4,027 ha and encompasses the small basin as well as the densely forested upstream areas of the dam.

Fig. 1 The study area



2.2 Satellite imagery

To investigate land use and vegetation cover changes over 30 years and to assess the impact of dam construction on regional land use, two satellite images were utilized: one from Landsat 5 captured before the dam’s construction and one from Sentinel-2 captured approximately 20 years after the dam

became operational. The timing of image acquisition was selected such that both images were taken during the same summer month. This approach aimed to minimize variations in vegetation reflectance (Senseman et al., 1996) and to ensure that the selected season provided the most accurate and reliable results. The specifications of the satellite images used in this study are presented in Table 1.

Table 1 Information of the satellite images used. (U.S. Geological Survey, 1991; U.S. Geological Survey, 2021)

Satellite name	sensors	Imaging time	Pass number and Row	Spatial resolution(m)	Number of bands
Landsat 5	TM	1991/08/28	165/35	30	7
Sentinel 2B	MSI	2021/09/02	T39v	10	13

2.3 Satellite Image Preprocessing

Before the utilization of raw satellite imagery, a series of preprocessing steps was applied to digital images. These procedures aim to convert the recorded light intensity values into reflectance or radiance values, which are known as Digital Numbers (DN). To reduce image-related errors, the FLAASH algorithm was applied after delineating the selected regions. All preprocessing and processing steps for the multispectral images were conducted using ENVI5.6 software. Radiometric, atmospheric, and geometric corrections were applied solely to the Landsat 5 imagery. Sentinel-2B images were obtained from Sentinel-related platforms and websites, and were already preprocessed using radiometric correction, atmospheric correction, and orbital correction methods, the latter of which offers higher geometric accuracy and prepares the data for analysis.

2.4 Delineation of the study area

In selecting the study area for the present research, aerial maps and the Digital Elevation Model (DEM) of the region were utilized. Using ArcGIS software and the Arc Hydro toolset, the hydrological network of the region was identified to ensure that the dam site and its surrounding significant forest and rangeland areas were encompassed within a broader

watershed. Two spatial scales were selected for analysis. The smaller watershed is located between approximately 36° 15' to 36° 20' E longitude and 26° 10' to 26° 15' N latitude. This area includes the immediate surroundings of the Meyjaran Dam, parts of dense forests, and the zones directly affected by reservoir impoundment. The larger watershed extends from approximately 36° 05' to 36° 47' E longitude and 26° 04' to 26° 57' N latitude. This area covers the entire upstream watershed draining into the dam and includes forests, rangelands, agricultural lands, and residential zones.

2.5 Research Methodology

Following the acquisition of satellite images, implementation of the necessary preprocessing steps, and delineation of the study area, the images were clipped according to the defined boundaries. To analyze land use and land cover classes and their changes over time, it was necessary—based on literature review, resource assessment, and field visits—to determine both the number of classes and the appropriate label for each. Subsequently, a supervised classification approach was employed using the Maximum Likelihood method for land use classification.

Supervised classification, which is based on selecting training samples for each class and comparing all other pixels against

these reference samples, is considered a reliable approach (Richards et al., 2022). After identifying and selecting training samples for each class, land use maps for the years 1991 and 2021 were generated using the Maximum Likelihood method in ENVI 5.6 software. Due to the unique topographic and environmental characteristics of the region, other supervised classification methods—including Support Vector Machine (SVM), Neural Networks, and Minimum Distance—were also tested. However, the parametric Maximum Likelihood method yielded the most accurate classification results for this study.

2.5.1 Maximum likelihood method

This is a parametric supervised classification method based on Bayes' theorem, which classifies pixels using variance and covariance matrices. Each pixel is assigned to the class for which it has the highest probability of membership (Alavi Panah, 2003).

Maximum Likelihood classification is sensitive to the number of training samples (Sengupta et al., 2024). In cases where a pixel is located near the boundary of two classes and exhibits an equal probability of belonging to either, it will be assigned to the class with the greater number of training samples. Therefore, it is crucial to select a balanced number of training samples across all classes (Beleites et al., 2013).

2.5.2 Map generation

To generate land use maps and calculate the area of each land cover class and feature, the classification results obtained using the Maximum Likelihood method were first processed in ENVI 5.6. These results were then saved in shapefile or TIFF format for further analysis in ArcMap. In the subsequent step, using ArcMap 10.8, the *Dissolve* operation was performed, and the area of each land use class within the respective watersheds for the two study years was calculated. A comprehensive classified map with a corresponding legend table was also produced in the same software.

2.5.3 Change detection map generation

To detect land use and vegetation cover changes, the *Change Detection* module of ENVI 5.6 software was utilized. This was carried out by comparing the two classified maps from 1991 and 2021, providing a visual and graphical representation of the changes over the 30-year period.

2.6 Spatial pattern change analysis using the location quotient index

To conduct a more precise analysis of spatial changes and to calculate the concentration and contribution of different land use change types, the Location Quotient (LQ) index, also known as LQ statistical analysis, was employed. The LQ index reveals which land use type has had the most significant impact within each sub-watershed. This method serves as a metric designed to determine the relative share of the area occupied by a given land use class within a specific sub-region compared to other sub-regions within the broader study area. In this study, land use areas for the years 1991 and 2021 were compared across two watersheds (small and large) to identify the concentration of land use changes over the 30-year period. The Location Quotient index is defined by Eq. 1 (Shahiki et al., 2019):

$$LQ = \frac{(A_i/A_t)}{(B_i/B_t)} \quad (1)$$

where, LQ denotes the Location Quotient index, where (A_i) represents the area of a specific land use type within a sub-region, (A_t) is the total area of that land use type across the entire study area, (B_i) denotes the total area of the sub-region under consideration, and (B_t) is the total area of the study region. An LQ value of less than 1 indicates that the concentration of a particular land use in each sub-region is lower than in other parts of the study area. An LQ value close to 1 reflects a balanced distribution of that land use across the region. Conversely, an LQ greater than 1 indicates a higher concentration of that land use type in the sub-region compared to others, suggesting that the most significant land use changes have occurred in that area (Shahiki et al., 2019).

2.7 Evaluation of classification performance and methodology for land use change detection

Overall accuracy serves as a key metric for evaluating the performance of classification, calculated by dividing the sum of the diagonal elements of the error matrix by the total number of pixels. The Kappa coefficient is a statistical index derived from the error matrix that measures the agreement between the classified data and a random classification. The Kappa coefficient is defined by Eq. 2 (Asghari et al., 2020):

$$K = \frac{(P_o - P_e)}{(1 - P_e)} \quad (2)$$

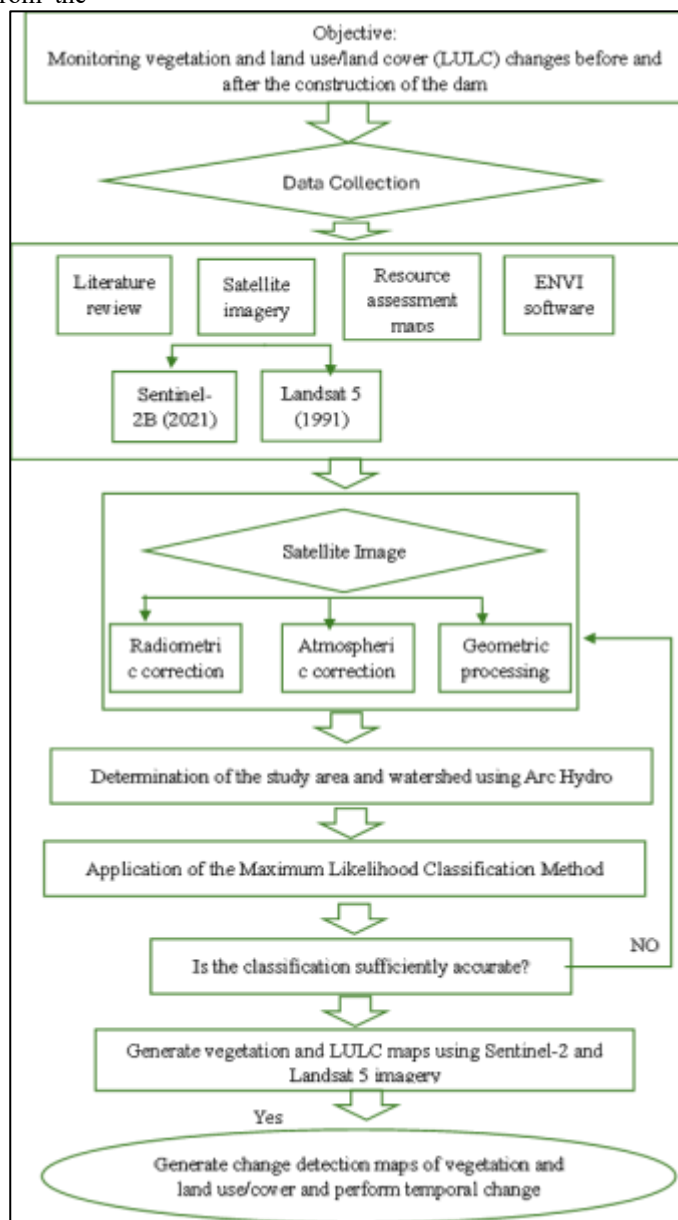
where, K denotes the Kappa coefficient, where (P_o) is the observed overall accuracy from the error matrix and (P_e) represents the expected accuracy from random chance. In remote sensing and Geographic Information System (GIS) studies, various methods exist for detecting land use and land cover changes. Among them, the post-classification comparison method was selected in this study for analyzing the environmental impacts of the construction of the Meyjaran Dam. In this method, each satellite image was classified independently, and then the classification results were compared. This approach enabled the precise identification of changes between land use classes. Due to the use of different satellite images such as Landsat 5 and Sentinel-2 across various time intervals, the post-classification comparison method was effective in minimizing the influence of sensor differences and atmospheric conditions, thereby yielding more reliable results.

The resulting land cover change maps were presented as change matrices, which facilitated the interpretation and analysis of changes. Additionally, this approach allowed for the calculation of statistical indices such as overall accuracy and the Kappa coefficient to evaluate the reliability of the results. Given these advantages, the post-classification comparison method was selected as an effective technique for detecting land use and land cover changes in this study. To enhance the accuracy of the results, geometric and radiometric corrections were applied to the satellite images. The images were cropped to the study area, covering an area of 145 km². Training samples for each land use class were carefully selected, and the number of samples was standardized to approximately 120 per class. Several classification methods were tested, and the Maximum Likelihood Classification method was ultimately chosen due to its superior accuracy of

92%. The error matrix was computed, and a Kappa coefficient of 0.89 was obtained.

The LQ index was employed to analyze spatial changes under an ambient temperature condition of 18°C. The results indicated that approximately 35% of the land around the dam had undergone land use changes, primarily occurring within a 2 km radius of the dam axis. To validate the results, field surveys were conducted, and the data collected were compared with the classification outcomes. Satellite images from the

Fig. 2 The step-by-step study execution process



For the Kappa coefficient (K), P_o represents the overall observed accuracy derived from the error matrix, while P_e indicates the expected accuracy under random classification conditions. In remote sensing and Geographic Information Systems (GIS) studies, various methods exist for detecting land use and vegetation cover changes. Among these, the post-classification comparison method was selected to analyze the environmental impacts resulting from the construction of the Meyjaran Dam. In this approach, each satellite image was independently classified, and the classified results were

subsequently compared. This process enabled accurate identification of changes between land use classes. Due to the use of different satellite images, such as Landsat 5 and Sentinel-2, acquired over different periods, the post-classification comparison method proved effective in reducing the influence of sensor disparities and atmospheric conditions. This contributed to producing more reliable results. The resulting change maps were presented in the form of a change matrix, which facilitated the interpretation and analysis of changes. Moreover, it allowed for the calculation of statistical

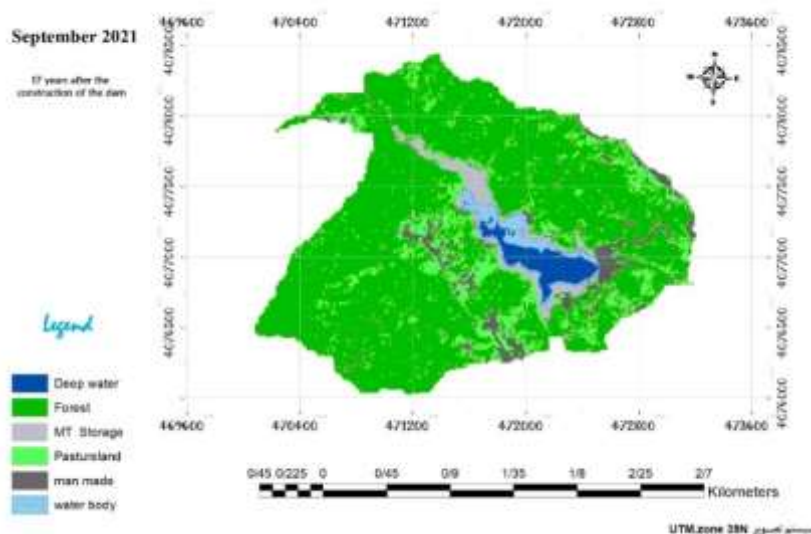
indicators such as overall accuracy and the Kappa coefficient to assess the reliability of the results. Given these advantages, the post-classification comparison method was selected as an effective approach for detecting land use and vegetation cover changes in this study.

2.8 Validation and spatial analysis of land use changes surrounding the Meyjaran Dam

To improve the accuracy of the results, geometric and radiometric corrections were applied to the images. The images were cropped to the study area, covering an area of 145 km². Training samples for each land use class were carefully selected, and their number was standardized to approximately 120 samples. Several classification methods were tested, and ultimately the Maximum Likelihood method was selected, achieving an accuracy of 92%. The error matrix was calculated, and a Kappa coefficient of 0.89 was obtained. The spatial autocorrelation index was used to examine spatial variations in ambient temperature at 18 °C. The results indicated that 35% of the land surrounding the dam had undergone land use changes, primarily occurring within a 2 km radius of the dam axis.

To validate the results, field visits were conducted, and the collected data were compared with the classification outcomes. Satellite images from the years 1991 and 2021 during the summer season were selected to minimize the influence of seasonal variation. A flowchart illustrating the research methodology is presented in [Fig. 2](#).

Fig. 3 The land use map of the study area in 2021



In the final land use map for the year 2021, presented in [Fig. 3](#), it was observed that due to the water storage conditions in the dam reservoir during September 2021, approximately 38.9% of the lake surface had dried up, with only a limited volume of water remaining relative to the reservoir's full capacity. The analysis of satellite images and the resulting maps from 1991, shown in [Fig. 4](#), reveals the cutting and submergence of many old-growth trees due to the construction of the dam, which ultimately led to their decay. Land use classes in 1991, before dam construction, were also categorized into four main types: forest cover, rangeland and

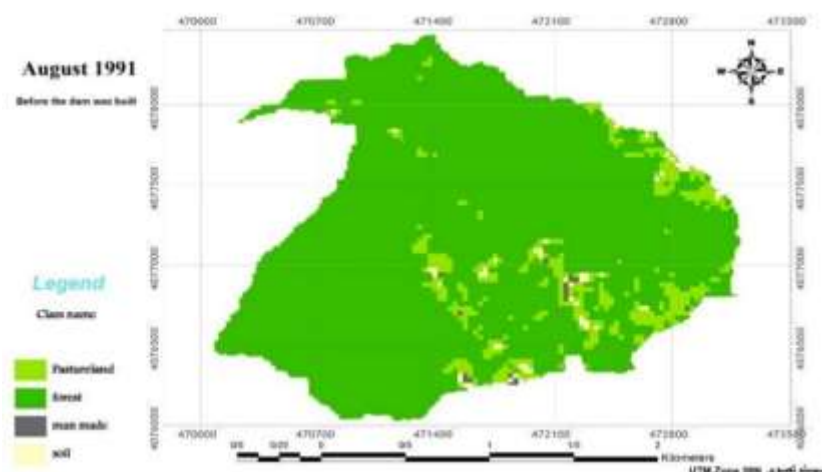
3. Results and Discussion

Under the study's objectives, the environmental conditions of the area, and the status of satellite imagery from the year 2021, the required land use classes for map production were categorized into four groups: forest cover; rangeland and agricultural areas; built-up areas including residential zones, roads, the dam structure, and recreational areas; and water bodies, encompassing the total area of shallow, deep, and dry sections of the dam reservoir. In 2021, the total area of the dam reservoir under study was 40 ha. This area was divided into three main sections. The dry section of the reservoir, covering 15 ha, represented the largest portion, accounting for 38.9% of the total area. This was followed by the deep-water section, with an area of 13ha, comprising 33.3% of the reservoir. The shallow water section, covering 11 ha, made up 27.8% of the total reservoir area ([Table 2](#)).

Table 2 Separation of the areas of each part of the water area of the studied area in 2021

Water Body Section	area (ha)	share of the total (%)
Deep water	13	33.3
Water	11	27.8
The empty part of the dam	15	38.9
Total (dam reservoir)	40	100

agriculture, bare soil, and built-up areas. In [Fig. 4](#), which represents the land use map derived from the 1991 Landsat 5 satellite image, it is evident that the current lake area of the dam consisted of multiple land cover types, including forest, rangeland, and a small built-up area. This residential or recreational area, located within the forest, was entirely converted into a water body following the dam's impoundment. Collectively, these three land use types, covering approximately 40 ha in 1991, were fully transformed into aquatic land use.

Fig. 4 The land use map of the study area in 1991

A comparison between Figs. 3 and 4 illustrate the extent of human intervention and the resulting environmental and ecological changes in the region over time. According to the accuracy assessment of satellite image classification, the kappa coefficient in 1991 was calculated at 0.92, with an overall accuracy of 95%. To ensure classification reliability, both the kappa coefficient and overall accuracy were evaluated, with values approaching 1.0, indicating high classification precision. In 2021, utilizing higher-resolution Sentinel-2B imagery and improved processing techniques, the kappa coefficient increased to 0.99, and the overall accuracy reached 99%. These values confirm the high precision and

reliability of the supervised classification method using the maximum likelihood algorithm.

During this process, although approximately 40 ha of forest and rangeland were initially degraded, over the 30 years, nearly 84 ha—equivalent to 18% of dense forest cover—were converted to rangelands, built-up areas, and water bodies due to dam construction, residential development, road expansion, and tourism infrastructure. Additionally, the reduction in bare soil land use is likely associated with the conversion of dirt roads into paved roads, which in 2021 were classified as part of the built-up areas.

Table 3 Comparison of land use areas and percentages in the study area and watershed for 1991 and 2021

Land use type	Study area						Entire Watershed					
	1991		2021		Change		1991		2021		Change	
Area	(ha)	%	(ha)	%	(ha)	%	(ha)	%	(ha)	%	(ha)	%
Forest	418	90	334	72	-84	-18	3869	96.1	37481	93.1	-121	-3
Pastureland	39	8.5	63	13.7	24	5.2	120	3	156	3.9	37	0.9
Man-made	2	0.4	27	5.8	25	5.4	9	0.2	74	1.9	659	1.1
Water bodies	0	0	40	8.5	40	8.5	0	0	40	0.99	40	0.99
Bare soil	5	1.1	0	0	-5	-1.1	29	0.7	8.62	0.2	-20	-0.5
Total	464	100	464	100	—	—	4027	100	4027	100	—	—

Positive values indicate an increase, while negative values represent a decrease.

Land use changes based on the LQ index were also assessed over the study period, with the results presented in [Table 4](#). In the smaller study area, forest concentration declined from 0.9 in 1991 to 0.8 in 2021. The LQ for rangelands increased from 2.8 to 3.5, and for built-up areas, from 1.6 to 3.2. In the larger watershed, the LQ for forest remained relatively stable, while the concentration of rangelands and built-up regions decreased. The construction and operation of a dam covering approximately 40 ha over 30 years has had significant environmental impacts on the surrounding small watershed.

Table 4 Changes of spatial coefficients for each user in 1991 and 2021

land use	LQ index of 1991		LQ index of 2021	
	Area 1	Area 2	Area 1	Area 2
forest	0.94	1	0.78	1.03
Pastureland	2.85	0.76	3.53	0.67
Man-made	1.64	0.92	3.16	0.72
water body	0	0	8.67	0

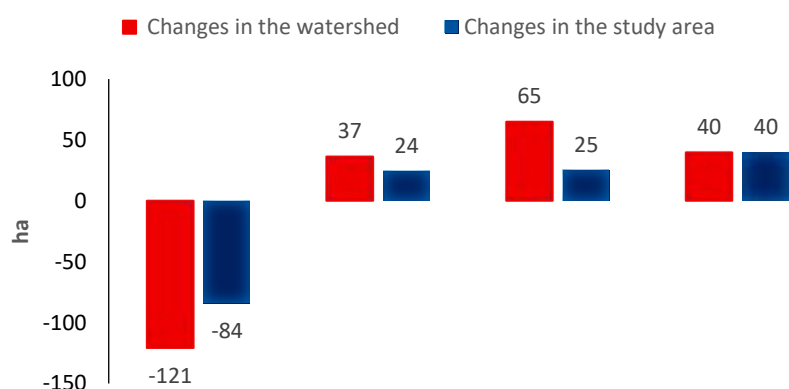
In the larger watershed, the overall changes follow a similar trend, including a reduction of 121 ha (3%) in forest cover and an increase of 65 ha in built-up areas. However, it is important to note that at the most detailed level, such changes may vary due to differences in hydro-aquae-pedologic conditions. The magnitude and significance of forest cover loss in the study area can be illustrated by the case of the Dalkhani Forest, which constitutes part of the smaller watershed within the study area and covers approximately 60 ha. Nevertheless, the extent of forest degradation and loss across the broader region exceeds 120 ha, meaning that nearly twice the area of the Dalkhani Forest has been deforested. Regarding the Location Quotient (LQ) table ([Table 3](#)), the smaller watershed covering approximately 464 ha and located around the dam is shown in [Fig. 6](#). Watershed 2 is derived by subtracting the smaller watershed from the larger one (i.e., larger watershed – smaller watershed). The purpose of calculating the LQ for the larger watershed was to assess spatial changes independent of the smaller watershed and its associated alterations. For instance,

land use concentration and equilibrium in the larger watershed (excluding the smaller watershed) have consistently favored forest cover.

The results indicated that in the larger watershed (excluding the smaller watershed), forest land use consistently remained dominant, with an LQ of 1.00 in 1991 and 1.03 in 2021, reflecting a stable concentration of forest cover in this area. The highest LQ in 2021 was recorded for the water body class in the smaller watershed, which showed a high level of spatial concentration due to the construction of the dam and its

associated changes. According to the LQ values for Watershed 1 in 1991 and 2021, it was observed that over the 30 years, rangeland, agricultural land, and built-up areas experienced an increase, as indicated by the rising LQ values. This increase may be attributed to the expansion of human activities such as agriculture, construction, and land-use transformation. [Fig. 5](#) illustrates the environmental impact of the Meyjaran Dam. The sharp decline in forest cover and the increase in built-up areas and water bodies can be attributed to tree felling, submergence of forested areas, the expansion of infrastructure, and the development of structures related to the dam project.

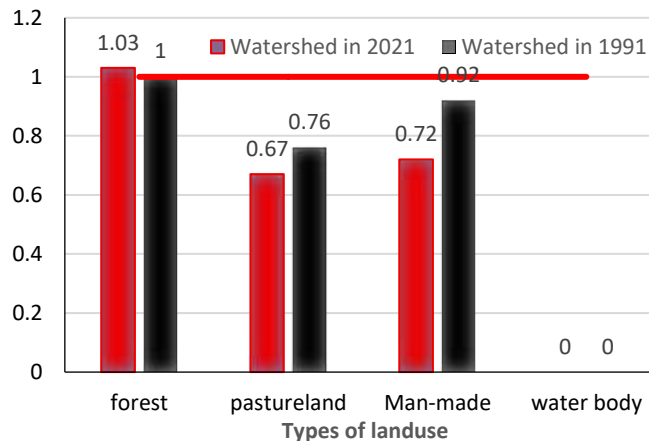
Fig. 5 Chart of changes in the area (ha) of the watershed and the study area between 1991 and 2021



As illustrated in Figs. 6 and 7, the most significant changes relating to the area of each zone pertain to built-up areas. These changes are primarily attributed to dam construction and the development of a tourist region, which has led to a marked increase in infrastructure, including roads, accommodations,

recreational facilities, and residential villas. An analysis of land use and vegetation cover changes in the study area from 1991 and 2021 reveals substantial transformations in both the smaller and larger watersheds.

Fig. 6 Comparison of the spatial coefficient of vegetation and types of land uses in the studied watersheds in 1991 and 2021

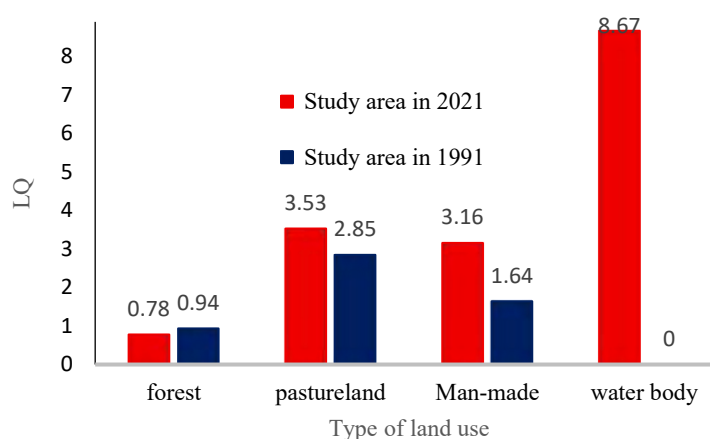


In the small watershed (464.25 ha), a decrease of 84.22 ha (18.4%) of forest cover was observed over a period of 30 years, while the area of rangelands and agricultural lands increased by 24.19 ha (5.21%) and built-up areas increased by 25.25 ha (5.44%). A new body of 39.67 ha (8.54%) was also created in 2021, which did not exist previously. A study in the vicinity of the Sahand Dam indicated that dam construction led to significant changes in land use and a reduction in ecosystem services (Nouri et al., 2018). Similarly, investigations around the Karun Dam revealed changes in land use, a decrease in vegetation cover, and an increase in urban areas after the construction of the dam (Baluchi et al., 2016). Another study showed that the construction of the Alborz Dam caused

significant changes in vegetation cover and land use, especially in the upstream section of the dam (Darikandeh et al., 2020).

In the larger watershed (4026.99 ha), a reduction of 120.80 ha (3%) of forests was recorded. The area of rangelands and agricultural lands increased by 36.28 ha (0.9%), and built-up areas expanded by 65.05 ha (1.61%). A new water body of 39.68 ha (0.99%) was created in 2021 in the larger watershed. These results are consistent with similar studies. For instance, a study on the impact of the construction of the Mulla Sadra Dam on land use changes showed an increase in agricultural land area upstream and a decrease downstream of the dam (Kamali & Didari, 2024).

Fig. 7 Comparison of the spatial coefficient of vegetation cover and types of land uses in the studied areas in 1991 and 2021



The Land Use Concentration (LQ) indices showed that, in the small watershed, the spatial concentration of forests decreased, while the spatial concentration of rangelands and built-up areas increased.

4. Conclusion

The construction and impoundment of large dams, while potentially meeting the demands for drinking water, agriculture, and tourism, can lead to the destruction and degradation of forest cover in areas with rich and dense vegetation, resulting in the extinction of rare plant species, wildlife, and animal ecosystems. The main objective of this study was to analyze land use changes in the area surrounding Meyjaran Dam in 1991 and 2021 using satellite imagery and to assess the impact of dam construction on these changes. This study was conducted using remote sensing and GIS methods. The main findings of the research are as follows:

1. Forest destruction around the dam reached 84 ha, and in the sub-basin under study, it exceeded 120 ha, indicating negative impacts beyond expectations.
2. The evaluation of the Kappa coefficient and the classification accuracy of the satellite imagery for 1991 were 0.9216 and 0.9459, respectively, and for 2021, they were 0.9901 and 0.9927, reflecting the accuracy and precision of the classification.
3. Increase in water and built-up areas: The construction of the dam resulted in an increase of 39.67 ha in water bodies and 25.25 ha in built-up areas. Additionally, the area of rangelands increased by 24.19 ha, although a decrease was observed near the dam.

The difference in spatial resolution between the old and new satellite images was identified as a limiting factor in the accuracy of comparisons. The lack of access to precise field data from the years prior to dam construction was also considered another limitation of the study. To simulate future land use changes, the use of predictive models such as CA-Markov or LSTM is recommended. Continuous monitoring of the area using high-resolution satellite imagery is suggested for managing the environmental impacts of the dam. Finally, it is recommended that the long-term environmental impacts, especially in areas rich in vegetation, be thoroughly assessed and considered when constructing large dams. The results of this study emphasize the need for comprehensive environmental assessments before the construction of large

dams and the sustainable management of natural resources in sensitive areas.

Statements and Declarations

Data Availability

The data are presented within the manuscript. Upon request, supplementary data can be provided by the corresponding author via email.

Conflicts of interest

The authors of this paper declared no conflict of interest regarding the authorship or publication of this article.

Author contribution

M. Golbaf: Study design, image acquisition, preprocessing and processing of satellite images, calculation of statistical indices (LQ spatial coefficient and Kappa coefficient), satellite data analysis, supervised classification using maximum likelihood method, change detection map production, manuscript drafting. F. Papoli Yazdi: Delineation and extraction of watershed boundaries, examination of land use changes, production of location maps, and contribution to the analysis of results and manuscript writing. F. Modaresi: Study design, oversight of research execution, analysis of results, manuscript editing, and final review of the research.

AI Use Declaration

This study did not incorporate artificial intelligence techniques; instead, all analyses and optimizations were conducted using conventional and widely accepted analytical methods.

References

- Alavi Panah, M. (2003). Remote Sensing and Geographic Information System. University of Tehran Press, Tehran. 311 p. [In Persian].
- Almalki, R., Khaki, M., Saco, P. M., & Rodriguez, J. F. (2023). The impact of dam construction on downstream vegetation areas in dry areas using satellite remote sensing: A case study. *Remote Sensing*, 15(21), 5252. <https://doi.org/10.3390/rs15215252>
- Asghari, S., Jalilyan, R., Pirozineghad, N., Madadi, A., & Yadeghari M. (2020) Evaluation of water extraction indices using landsat satellite images (Case study:

- Gamasiab River of Kermanshah). *Journal of Applied Research in Geographical Sciences*, 20(58), 53-70. doi:[10.29252/jgs.20.58.53](https://doi.org/10.29252/jgs.20.58.53) [In Persian].
- Baluchi, B., Dehghani, M., & Nikoo, M. R. (2016). Assessing land-use change induced by the Karkhe Dam using satellite images and maximum likelihood classification method. *Scientific Quarterly of Water Resources Engineering*, 9(28), 19-32. [20.1001.1.20086377.1395.9.28.2.3](https://doi.org/20.1001.1.20086377.1395.9.28.2.3) [In Persian]
- Beleites, C., Neugebauer, U., Bocklitz, T., Krafft, C., & Popp, J. (2013). Sample size planning for classification models. *Analytica Chimica Acta*, 760, 25–33. <https://doi.org/10.1016/j.aca.2012.11.007>
- Castro-Diaz, L., Lopez, M. C., Moore, S., Radonic, L., Hodbod, J., & Moran, E. (2024). Multidimensional and multitemporal energy injustices: Exploring the downstream impacts of the Belo Monte hydropower dam in the Amazon. *Energy Research and Social Science*, 113, 103568. DOI:<https://doi.org/10.1016/j.erss.2024.103568>
- Darikandeh, D., Ghorbani, D., & Shahnazari, A. (2020). Monitoring changes caused by the construction of the alborz dam on land cover and land use through remote sensing and geographic information systems. *Journal of Watershed Management Research*, 11(21), 24-35. DOI:[10.52547/jwmr.11.21.24](https://doi.org/10.52547/jwmr.11.21.24)
- Kamali, M., & Didari, S. (2024). Investigating the effects of constructing the Mulla Sadra Dam and land use changes on water resources in downstream basins. *Proceedings of the First National Conference on the Future and Sustainability of the Environment*, Tehran. <https://civilica.com/doc/2112502> [In Persian]
- Linh, H. T., Truc, D. T., Binh, N. T., & Tri, V. P. D. (2025). Assessing water governance trends and challenges at a local level—an application of the OECD water governance framework in Soc Trang Province, Vietnam. *Water*, 17(3), 320. <https://doi.org/10.3390/w17030320>
- Motkan, A.A., Saeedi, K.H., Shakiba, A. & Hoseini Asl, A. (2010). Evaluation of land cover changes in relation to Taleghan Dam using remote sensing techniques. *Journal of Applied Geosciences Research*, 16(19): 45-64, <http://jgs.khu.ac.ir/article-1-610-fa.html> [In Persian].
- Namdar, F., Mahmoudi, S., Esmali Ouri, A., & Pazira, E. (2021). Monitoring of Thirty Years of Land Cover Changes Using Remote Sensing and GIS (Case Study: Qaresu Watershed, Ardabil). *Journal of Environmental Science and Technology*, 22(12), 179-190. Doi: [10.22034/jest.2020.45905.4755](https://doi.org/10.22034/jest.2020.45905.4755) [In Persian].
- Ouma, Y. O., Nkwae, B., Odirile, P., Moalafhi, D. B., Anderson, G., Parida, B., & Qi, J. (2024). Land-use change prediction in dam catchment using logistic regression-CA, ANN-CA, and random forest regression and implications for sustainable land–water nexus. *Sustainability*, 16(4), 1699. <https://doi.org/10.3390/su16041699>
- Richards, J. A. (2022). Supervised classification techniques. In: *Remote sensing digital image analysis*, Springer, Cham. 263-367. https://doi.org/10.1007/978-3-030-82327-6_8
- Sanjari, S., & Boroomand, N. (2013). Land Use/Cover Change Detection in Last Three Decades Using Remote Sensing Technique (Case Study: Zarand Region, Kerman Province). *Journal of RS GIS for Natural Resources*, 4(1), 57-67. <https://sid.ir/paper/189604/fa> [In Persian].
- Sengupta, D., Klein, S., Raine, J. A., & Golling, T. (2024). CURTAINS flows for flows: Constructing unobserved regions with maximum likelihood estimation. *SciPost Physics*, 17(2), 046. <https://doi.org/10.21468/SciPostPhys.17.2.046>
- Senseman, G. M., Bagley, C. F., & Tweddle, S. A. (1996). Correlation of rangeland cover measures to satellite-imagery-derived vegetation indices. *Geocarto International*, 11(3), 29–38. <https://doi.org/10.1080/10106049609354546>
- Shahiki Taash, M. N., & Roodini, K. (2019). Measuring the geographical concentration factor of factory industries and the importance of industrial specialization in the provinces of Iran. *Geography and Regional Urban Planning*, 9(31), 173–196. <https://doi.org/10.22111/gaij.2019.4711>
- Thakkar, A. K., Desai, V. R., Patel, A., & Potdar, M. B. (2017). Impact assessment of watershed management programs on land use/land cover dynamics using remote sensing and GIS. *Remote Sensing Applications: Society and Environment*, 5, 1-15. <https://doi.org/10.1016/j.rsase.2016.12.001>
- U.S. Geological Survey. (1991, August 28). *Landsat 5 TM image, Path 165, Row 35* [Satellite image]. USGS EarthExplorer. <https://earthexplorer.usgs.gov>
- U.S. Geological Survey. (2021, September 2). *Sentinel-2B MSI image, Tile T39V* [Satellite image]. USGS EarthExplorer. <https://earthexplorer.usgs.gov>
- Yu, H., Zahidi, I., Fai, C. M., Liang, D., & Madsen, D. Ø. (2025). Tailings dam failures: A critical evaluation of current policies and practices. *Results in Engineering*, 25, 103973. <https://doi.org/10.1016/j.rineng.2025.103973>
- Zarei, H., Shanani Hoveyze, S. M., & Joorabian Shooshtari, S. (2024). Temporal-Spatial Prediction of Land Use Changes Using LCM Model in Doroodzan Dam Watershed. *Environment and Water Engineering*, 10(3), 363-378. <https://doi.org/10.22034/ewe.2023.408348.1881> [In Persian].



© Authors, Published by *Environ. Water Eng.* Journal. This is an open-access article distributed under the CC BY (license <http://creativecommons.org/licenses/by/4.0>).